ACS APPLIED MATERIALS & INTERFACES

Research Article

www.acsami.org

Role of the Surface Chemistry of Ceria Surfaces on Silicate Adsorption

Jihoon Seo,[†,⊥] Jung Woo Lee,[†,⊥] Jinok Moon,[†,‡] Wolfgang Sigmund,[§] and Ungyu Paik[†,*]

[†]Department of Energy Engineering, Hanyang University, Seoul 133-791, South Korea

[‡]Clean/CMP Technology Team, Memory, Samsung Electronics, Gyeonggi-Do 445-701, South Korea

[§]Department of Materials Science and Engineering, University of Florida, Gainesville, Florida 32611, United States

Supporting Information

ABSTRACT: Ceria nanoparticles (NPs) have been widely explored as a promising material in various fields. As synthesized under various physicochemical conditions, it exhibits the different surface chemistry. Here, the role of hydroxyl and nitrate group on ceria surface, formed under various physicochemical conditions, for the silicate adsorption was experimentally and theoretically investigated based on the adsorption isotherms and theoretical analyses using density functional theory (DFT) calculation. Experimental results acquired from adsorption isotherms with Freundlich model indicated that the nitrate group shows a much higher affinity with silicate than the hydroxyl groups. These phenomena were demonstrated through the theoretical approaches that exhibit the binding energy of the NO_3−ceria (−4.383 eV) on the SiO_2 surface being much higher than that of the OH−ceria (−3.813 eV). In good agreement with the experimental and the theoretical results based on adsorption properties, the results of chemical mechanical planarization (CMP) also show that the nitrate groups significantly enhance the removal of SiO_2 than the hydroxyl groups. The results investigated in this study will provide researchers, studying the ceria NPs, with guidelines on the importance of exploring the surface chemistry of ceria.

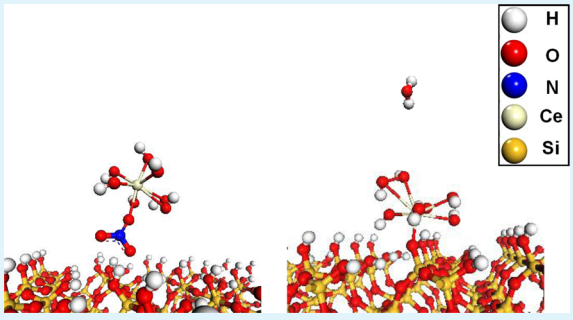

KEYWORDS: *ceria, surface chemistry, adsorption isotherm, DFT, calculation, CMP*

1. INTRODUCTION

As a promising material, ceria has received significant interest in various field including the water−gas shift reaction,[1,2] gas sensors,[3] fuel cells,[4,5] UV blocking,[6] and chemical mechanical planarization (CMP)[7] due to its the low redox potential. Ceria nanoparticles (NPs) can be synthesized via hydrothermal,[8,9] solvothermal,[10] precipitation,[11] thermal decomposition,[12] and sol-gel.[13,14] Although the shapes and sized of ceria NPs is similar as various synthesis methods, their physicochemical properties are quite different.[15−18]

Ceria NPs in the aqueous medium are sensitive to the changes in their physicochemical conditions including pH, ionic strength, temperature, and concentration,[19] which have influence on their agglomeration.[20] In the case of NPs of size less than 100 nm, they are extremely sensitive to changes in their physicochemical environments due to the higher surface energy of NPs than that of larger particles.[21] Ceria NPs, synthesized under various physicochemical conditions, exhibit different isoelectric points (IEPs) from pH 5.2 to 11.2.[15−18] The difference in the IEP values which varied with physicochemical conditions was interpreted through various ways in the literature.

The hydroxyl groups, one of the most common functionals, can be generated on the ceria surface by dissociation reaction of H_2O on defect site[22−24] or by protonation of outermost oxygens of the surface in acid solution.[25] Generally, ceria is functionalized with the hydroxyl groups in aqueous medium. However, ceria inevitably containing large concentrations of nitrate ions which originated from the precursor such as cerium nitrate hexahydrate induces the covalently bound nitrate groups on the ceria surface.[15] Although both the hydroxyl and nitrate group play an important role in the surface chemistry of ceria, there has been no reports related to the effect of surface chemistry of ceria on the adsorption behavior of anion.

Here, we have experimentally and theoretically investigated the effect of the hydroxyl and nitrate group on the ceria surface, formed under various physicochemical conditions, on the adsorption behavior of silicate as anion. To focus on the impacts of surface chemistry of ceria, other variables, the size and shape, were kept constant by preparing solution-grown ceria (NO_3-ceria) and ion-exchanged solution-grown ceria (OH-ceria). To elucidate the interaction between ceria and silicate, adsorption isothermal analysis of silicate on ceria were performed. As the results of adsorption isothermal analysis with the Freundlich model, the NO_3−ceria exhibits much higher affinity with silicate than the OH−ceria. An associated quantum

Received: February 7, 2014
Accepted: April 15, 2014
Published: April 15, 2014

mechanical study using density functional theory[26] to elucidate the role surface chemistry of ceria shows that NO_3−ceria has much higher binding energy with SiO_2 film than that of OH−ceria. As one of applications of ceria NPs, they has been widely used for chemical mechanical planarization (CMP) due to its remarkable characteristics including high SiO_2 removal rate.[27] The evaluation of CMP shows that the removal amount of SiO_2 film of the NO_3−ceria is 1.3 times higher than that of the OH−ceria. These results are well-correlated with the experimental results based on adsorption isotherms and the theoretical analyses using DFT calculation.

2. EXPERIMENTAL SECTION

Materials. An aqueous dispersion of solution-grown ceria (d_{mean} ∼ 60 nm, France) was obtained from Rhodia Inc. TEM images of ceria nanoparticles are shown in Figure S1 in the Supporting Information. To replace nitrate group with hydroxyl group, the suspensions were adjusted to pH 10.5. After aging, these were centrifuged during 20 min at 30000 rpm. The supernatant was decanted, and solids were redispersed in deionized water. This procedure was repeated several times to remove impurities. Finally, ceria was dried in an oven over 6 h at 110 °C. The specific surface area, measured via Brunauer−Emmett−Teller (BET) method using N_2 gas adsorption at 77K (Autosorb-1, Quantachrome, Syosset, NY) of NO_3−ceria and OH−ceria are 15.0 and 13.4 m^2/g, respectively. Sodium metasilicate ($Na_2SiO_3{\cdot}9H_2O$) in deionized water was obtained from Sigma-Aldrich. The ionizable acrylic polymer, poly(acrylic acid) (PAA, Polysciences Inc.; M_w = 10000 g/mol) was used as dispersant for ceria. Blanket SiO_2 films were grown a 1.4 μm thickness on 8 inch diameter Si wafer by plasma-enhanced tetraethyl orthosilicate (PETEOS). Each of these 8 inch wafers were cut into several 6 cm × 6 cm pieces for polishing.

Suspension Preparation. NO_3−ceria and OH−ceria was dispersed at 1.0 wt % in deionized water, respectively. PAA was added to the suspension at a weight fraction of 2% versus ceria for a stable suspension. The pH was adjusted to 7.0. The suspension was aged for 12 h at room temperature using a mixer (Ball mill, Nanointech, Korea).

Characterization Methods. To identify the characteristics of ceria surface, fourier-transform infrared spectra were recorded with an FT-IR spectrometer (Nicolet 5700, ThermoElectron, Madison, WI, US) in the range 4000−500 cm^{-1}. Samples were prepared by mixing the dried ceria powders with KBr using agate mortar and pestle.

Ceria suspensions were prepared for electrokinetic analysis. Two identical suspensions were prepared for each ESA test. Separate acid (1.0 N HCl) and base (1.0 N NaOH) titrants were used to adjust the suspension pH, beginning at the natural pH and subsequently combined to generate a complete titration curve. For analysis of electrokinetic behavior, suspensions were prepared at a solids mass fraction of 1.0 % ceria powder with 0.01 M $NaNO_3$ solution. The electrokinetic curves of the ceria suspensions were determined by the electrokinetic sonic amplitude (ESA) technique (ESA-9800, Matec Applied Sciences, Hopkinton, MA) as a functional of pH. The ESA technique can be used to determine pH_{iep} during a titration with a high degree of accuracy. The details of this electroacoustic technique, its application to ceramic systems, and the estimated measurement precision were reported previously.[28]

The adsorption isotherm for silicate ion and PAA on ceria was determined at room temperature by the solution-depletion method using a inductively coupled plasma atomic emission spectroscopy (ICP-AES, Perkin−Elmer Optima 4300 DV, Waltham, MA) and total organic carbon analyzer (TOC-5000A, Shimadzu Corp, Kyoto, Japan), respectively. Ceria was dispersed at 1.0 and 5.0 wt % solid content in various concentrations of silicate ion and PAA solutions, respectively. The pH was adjusted to 7.0. Suspensions were equilibrated for 12 h under mixing. The suspensions were centrifuged, and the supernatant was filtered using a 0.02 μm Anotop 25 syringe filter and then analyzed using ICP and TOC. Results were corrected for a background value using a blank solution derived from a native ceria suspension in the absence of additives. The ICP and TOC values were converted to mass using an experimentally determined calibration curve. Adsorption isotherms were derived from the difference between the amount added and the amount remaining in the supernatants.

Computational Detail. For the ceria nanoparticle, functionalized with both of the nitrate and hydroxyl groups, adsorption on the SiO_2 surface was calculated at the density functional level of theory. Here, we used the (001) plane of SiO_2 with H-termination on the oxygen atoms to describe wet process of the experiment. In addition, the Ce atoms were octahedrally coordinated by oxygen related functionals for the calculation of functionalized ceria. The energy calculations were performed with PW91 method generalized gradient approximation (GGA) and plane wave model using CASTEP program.[26] The supercell of 30.000 Å × 9.956 Å × 13.896 Å was used for the calculation, which represents nanotube length along the tube axis as *c*. All atoms were described using Vanderbilt ultrasoft pseudopotentials and cutoff energy of 240 eV where the set of *k*-points used to expand the electronic wave function based on the Monkhorst−Pack scheme within 5.0 × 10^{-5} eV/atom of total energies convergence. The adsorption energies of functionalized ceria on the (001) SiO_2 were calculated by following equation, $E_b = E$[functionalized ceria + (001) SiO_2] − E[functionalized ceria] + E[(001) SiO_2].

CMP Field Evaluation. The CMP field evaluation was performed using slurries including NO_3−ceria and OH−ceria with and without PAA. The 6 cm × 6 cm pieces were polished for 1 min on CMP tool (POLI-300, G&P Tech. Inc., Korea) with an industry standard CMP pad (IC 1000/Suba IV, Rohm and Haas Electronic Materials, USA). The polishing test conditions are shown in Table S1 in the Supporting Information. The removal rate of each sample was determined by measuring before and after film thickness using ellipsometry (MM-16, Horiba Jobin Yvon, Longjumeau, France)

3. RESULTS AND DISCUSSION

Figure 1 shows the FT-IR spectrum of the NO_3−ceria and the OH−ceria. It is well known that the broad stretching band from

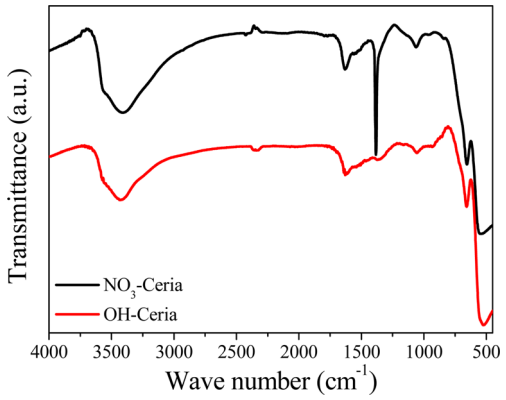

Figure 1. FT-IR spectra of NO_3−ceria and OH−ceria.

3200 to 3600 cm^{-1} corresponds to the hydroxyl groups, and the adsorption peaks at 400−750, 1640, and 1360 cm^{-1} presented on the surface of NO_3−ceria and OH−ceria correspond with the CeO_2 stretching frequency, the H_2O bending mode from the vapor phase condensation on a surface,[29,30] and Ce−OH stretching frequency, respectively.[31] The remarkable difference between the NO_3−ceria and OH−ceria is shown at 1380 cm^{-1} in the spectra, appearing in the strong stretching band. It is closely related to a nitrate group on the surface of ceria.[32,33] To focus on the impacts of the surface chemistry of ceria while other variables including the size and shape were kept constant, the nitrate group was replaced with hydroxyl group through the ion-exchange method. As pH increased, nitrate groups were

gradually released and entirely replaced by hydroxyl groups at pH above 10.5.[15]

$$Ce{-}O{-}NO_2 + OH^- \rightarrow Ce{-}OH + NO_3^- \quad (1)$$

The shift of the stretching band from 3408 to 3428 cm^{-1} in OH−ceria is shown due to the decrease of the absorption superposition between nitrate groups and hydroxyl groups by ion-exchange reaction.[34] And the strong stretching band at 1380 cm^{-1} disappeared in the spectra. This means that the nitrate group was successfully replaced with hydroxyl groups according to eq 1. Elemental analysis data also show that the N content was decreased by replacing a nitrate group with hydroxyl group and N was not observed in OH−ceria (see Table S2 in the Supporting Information). In the case of OH−ceria, the N content was not detected because the nitrate group of NO_3−ceria was replaced by a hydroxyl group. These results show that the surface chemistry of the ion-exchanged solution-grown ceria (OH−ceria) is similar to that of calcined ceria functionalized with the hydroxyl groups in the absence of chemisorbed or physisorbed species (see Figure S2 in the Supporting Information).

The electrokinetic behaviors of ceria particles with nitrate and hydroxyl group are shown in Figure 2. The IEP of NO_3−ceria occurs at pH 10.42. After replacing nitrate group with hydroxyl group according to eq 1, the IEP was shifted from 10.42 to 8.85.

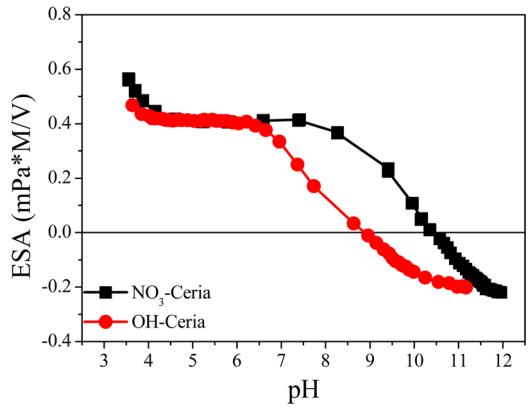

Figure 2. Electrokinetic behaviors of NO_3−ceria and OH−ceria as a function of pH.

This result indicates that the surface chemistry of OH−ceria is similar to that of calcined ceria in the absence of chemicsorbed or physisorbed species (see Figure S3 in the Supporting Information). The surface charge of ceria remains the same value since both nitrate ion and hydroxyl ion are monovalent state. We estimated that the nitrate group on the surface induced the increased hydration state since the IEP is strongly dependent on the state of hydration of the material surface.[18] As a result, the surface chemistry of OH−ceria became the same with that of calcined ceria in the absence of chemisorbed or physisorbed species by substituting nitrate group with hydroxyl group.

To elucidate the interaction between ceria and silica, adsorption isotherms of silicate ions on ceria were performed. Figure 3 and 4 show the adsorption isotherm of silicate ion on NO_3−ceria and OH−ceria at pH 7.0. The studies, related to the adsorption properties of the silicate ion on the ceria surface, are important since they directly correspond with CMP perform-

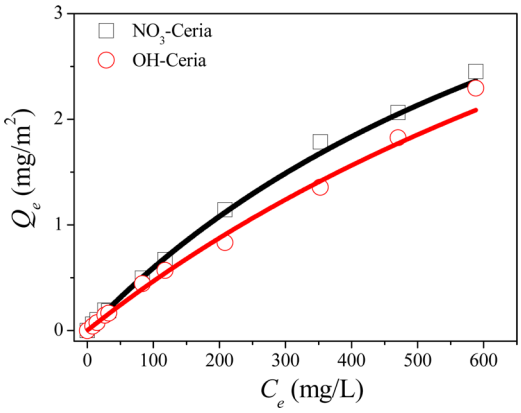

Figure 3. Langmuir plots for adsorption isotherm of silicate ion on NO_3−ceria and OH−ceria.

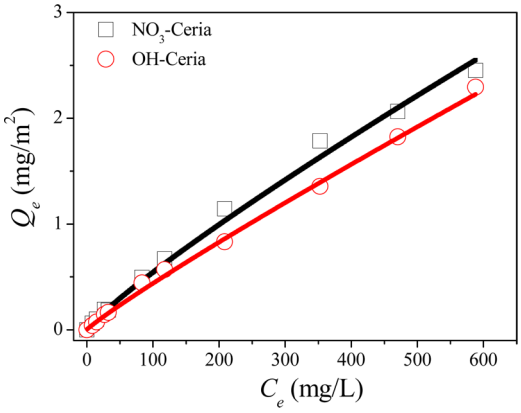

Figure 4. Freundlich plots for adsorption isotherm of silicate ion on NO_3−ceria and OH−ceria.

ance. However, there are few studies.[35,36] Hingston et al.[37−39] has studied the adsorption model of $Si(OH)_4$ as silicon ion that adsorbs on metal oxides. However, it may come to a good adsorption result in aqueous by complete speciation of the dissolved silicate species.[36] As a function of silicate ion concentration, the adsorbed amount of silicate ion on ceria was measured. Data of adsorption isotherms were fitted using Langmuir and Freundlich model.

The Langmuir adsorption isotherm model assumes that the silicate ion is homogeneously adsorbed on ceria surface by monolayer.[40] The Langmuir model is expressed by the following equation:

$$C_e/Q_e = C_e/Q_m + 1/(K_L Q_m) \quad (2)$$

Q_e is the adsorbed amount of silicate per specific surface area of ceria at equilibrium (mg/m^2), C_e is the concentration of silicate ion in the bulk solution (mg/L), Q_m is the maximum adsorbed amount (mg/m^2) of silicate on ceria surface, and K_L is related to the affinity of adsorption (L/mg).

The Freundlich adsorption isotherm model assumes that the silicate ion is adsorbed on ceria surface by heterogeneous systems. The Freundlich model is expressed by the following equation:

$$Q_e = K_F C_e^{1/n} \quad (3)$$

Q_e is the adsorbed amount of silicate ion per specific surface area of ceria at equilibrium (mg/m^2), C_e is concentration of

silicate ion in the bulk solution (mg/L). The Freundlich constant, K_F and $1/n$ is correlated a constant to the relative adsorption capacity and intensity of adsorption, respectively. The values of K_F and $1/n$ can be determined from the intercept and slope of linear plot of log Q_e versus log C_e.

$$\log Q_e = \log K_F + 1/n \log C_e \quad (4)$$

Table 1 shows the constants of the Langmuir and Freundlich isotherms. The higher correlation coefficient values (R^2) of the Freundlich model indicate that adsorption data of silicate ion on ceria are better fitted with the Freundlich isotherm model than the Langmuir isotherm model. The adsorption isotherm constants are important in understanding the interaction between ceria and SiO_2 film during CMP. A higher value of n indicates a higher affinity between adsorbate and adsorbent.[41]

Table 1. Langmuir and Freundlich Constants of Silicate Ion Adsorption on Ceria

	Langmuir constant			Freundlich constant		
	Q_m (mg/m^2)	K_L (L/mg)	R^2	K_F	n	R^2
NO_3–ceria	6.08	0.0011	0.8947	0.0097	1.1453	0.9973
OH–ceria	4.21	0.0009	0.7968	0.0064	1.0897	0.9971

As presented in Table 1, the K_F and n values of NO_3–ceria are higher with a silicate ion at pH 7 than those of OH–ceria. This indicates that a nitrate group on the surface induces ceria to high affinity with the silicate ion. Several researchers have reported that highly reactive sites such as Ce^{3+} species on the ceria surface have significantly influenced on the reaction with SiO_2.[42−44] The Ce(III)/Ce(IV) ratios of the NO_3–ceria and OH–ceria particles were evaluated using X-ray photoelectron spectroscopy (XPS). The Ce(III)/Ce(IV) ratios of the NO_3–ceria and OH–ceria particles are 0.085 and 0.119, respectively (see Figure S4 and Table S3 in the Supporting Information). The difference in the Ce(III)/Ce(IV) ratio between NO_3–ceria and OH–ceria is not significant due to a low concentration of Ce^{3+}. Thus, in this study, the surface chemistry such as nitrate and hydroxyl group have significantly influence on silicate adsorption.

On the other hand, various dispersants have been used to disperse ceria in aqueous media.[19,20,45,46] The anionic dispersant, poly(acrylic acid) (PAA), is widely used to disperse ceria nanoparticles in the CMP process since the insufficient repulsive forces between the abrasives and SiO_2 film surface can induce defects such as microscratches on the wafer surface.[47−49] Thus, the ceria nanoparticles are dispersed with PAA for CMP application. Figure S5 and S6 in the Supporting Information show the adsorption isotherm of PAA on NO_3–ceria and OH–ceria at pH 7.0. PAA has a carboxylic (−COOH) groups, which

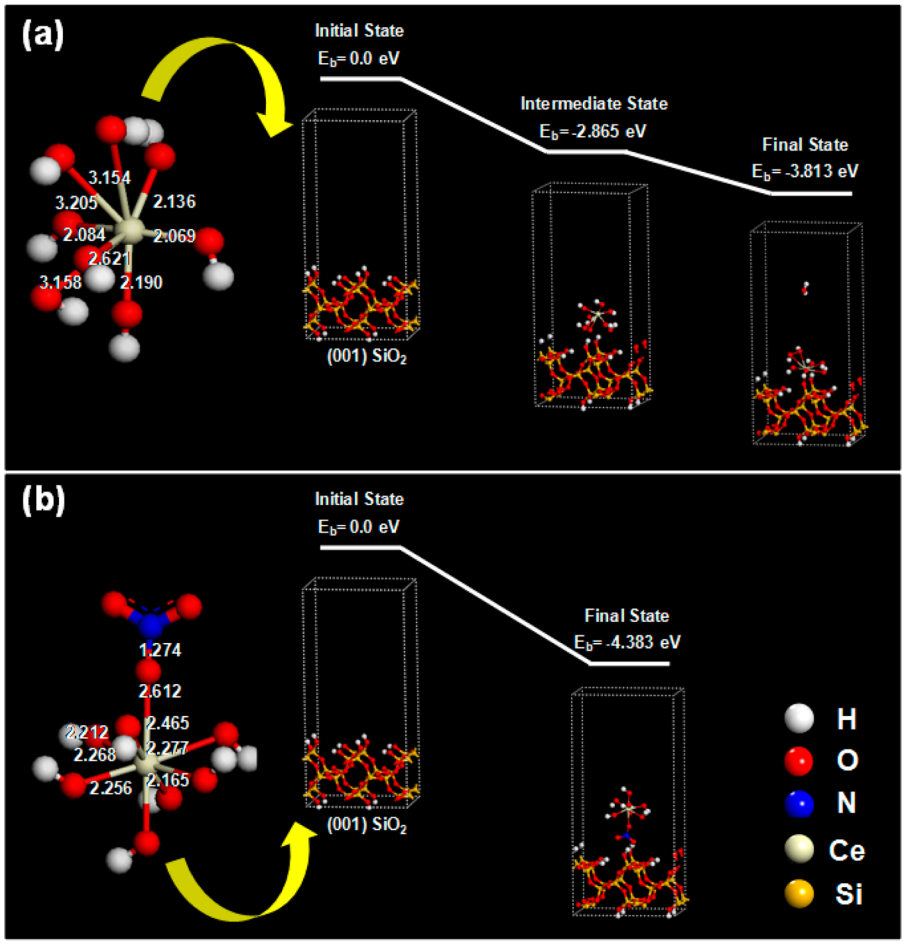

Figure 5. Fully optimized structures on the reaction of functionalized ceria adsorption on the SiO_2 (001) surface. (a) OH–ceria and (b) NO_3–ceria. The numbers indicate bonding length of two atoms near the Ce atom.

are deprotonated and becomes to negatively charged carboxylate ($-COO^-$) groups in aqueous with pH above its pKa of 4.5.[50] The adsorption of PAA on ceria surface can occur by the attractive force between negatively charged PAA and positively charged ceria. As shown in Supporting Information Table S4, the higher correlation coefficient values (R^2) of the Langmuir model indicate that adsorption data of PAA on ceria are better fitted with Langmuir isotherm model than Freundlich isotherm model. The maximum adsorbed amount, Q_m of NO_3−ceria and OH−ceria for monolayer coverage at pH 7 is 0.2247 and 0.2041 mg/m^2, respectively. The affinity of adsorption, K_L, of NO_3−ceria is higher than that of OH−ceria. This indicates that the nitrate group on the surface also induces ceria to high affinity with PAA.

To elucidate experimental adsorption inclination upon the functional groups, we have investigated the adsorption reaction at the molecular level through quantum mechanical calculation. First of all, we have used an octahedrally coordinated hydroxyl group and a nitrate group on the Ce atoms to describe the functionalized ceria nanoparticles (Figure 5a and b). The rest of the neighboring atoms were coordinated by a hydroxyl group for charge neutrality. In addition, the (001) SiO_2 was fully optimized with a single side open to represent the SiO_2 surface. Both of the sides were terminated by a hydrogen atom to describe wet chemical experiment conditions with the hydroxyl group and eliminate the end effect, respectively. The vacuum layer of the cell is set larger than 20 Å to minimize the interaction between the periodic structures (Figure 5a). In case of OH−ceria, two reaction steps could be considered. The first step is the OH−ceria adsorption on the H-terminated SiO_2 surface with electrostatic attraction force. Then, for the second step, the OH−ceria adsorption on the H-terminated SiO_2 surface is a water generating reaction. The binding energies of the both cases are −2.865 and −3.813 eV, respectively. On the other hand, only one step adsorption was considered for the NO_3−ceria without generating a water molecule (Figure 5b). The binding energy of this NO_3−ceria on the SiO_2 surface is much higher than that of the OH−ceria as −4.383 eV. This phenomenon might be due to the higher induced charge on the oxygen atom of the nitrate group. This theoretical result highly corresponds to the experimental data.

Figure 6 shows the effect of different surface chemistry on the surface on the CMP performance. The result shows that nitrate group on ceria surface induces an increased removal rate of SiO_2 film, which corresponds with the adsorption isotherm of silicate ion and theoretical analyses. NO_3−ceria with PAA also shows the higher SiO_2 removal rate due to an increased affinity and binding energy with silicate ion than that of OH-ceria with PAA.

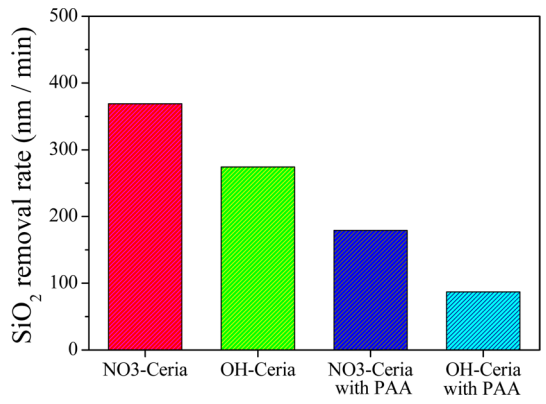

Figure 6. Removal rate of SiO_2 film of NO_3−ceria and OH−ceria at pH 7.0.

4. CONCLUSION

We demonstrated that surface functional groups including hydroxyl and nitrate groups have a significant influence on the adsorption properties of silicate ion on ceria surface. The adsorption data of silicate ion on ceria were fitted with Freundlich isotherm model. A K_F and n value among the constants of the Freundlich isotherms, related with affinity between ceria and silicate ion, indicated that NO_3−ceria shows higher with silicate ion at pH 7 than that of OH−ceria. Theoretical analyses using density functional theory (DFT) calculation exhibit the binding energy of the NO_3−ceria (−4.383 eV) on the SiO_2 surface is much higher than that of the OH−ceria (−3.813 eV). The experimental results and theoretical analysis indicate that the nitrate group on the ceria surface induces higher affinity and binding energy with silicate ions than the hydroxyl group, which is important for understanding the role of the surface chemistry of ceria during polishing and reaction between ceria and SiO_2 film. The results investigated in this study will provide researchers, studying applications using ceria, with guidelines on the importance of understanding the surface chemistry of ceria.

■ ASSOCIATED CONTENT

Ⓢ Supporting Information

Additional TEM, FTIR, ESA, XPS, and EA results of ceria. Adsorption isotherms of PAA on ceria. This material is available free of charge via the Internet at http://pubs.acs.org/.

■ AUTHOR INFORMATION

Corresponding Author

*E-mail: upaik@hanyang.ac.kr. Tel.: +82-2-2220-0502. Fax: +82-2-2281-0508.

Author Contributions

⊥Authors J.S. and J.L. contributed equally to this work.

Notes

The authors declare no competing financial interest.

■ ACKNOWLEDGMENTS

This work was supported by the Global Research Laboratory (GRL) Program (K20704000003TA050000310) through the National Research Foundation of Korea (NRF) funded by the Ministry of Science, ICT (Information and Communication Technologies) and Future Planning, and the International Cooperation program of the Korea Institute of Energy Technology Evaluation and Planning (KETEP) grant funded by the Korea government of Ministry of Trade, Industry & Energy (2011T100100369)

■ REFERENCES

(1) Fu, Q.; Saltsburg, H.; Flytzani-Stephanopoulos, M. Active Nonmetallic Au and Pt Species on Ceria-Based Water-Gas Shift Catalysts. *Science* **2003**, *301* (5635), 935−938.

(2) Pati, R. K.; Lee, I. C.; Hou, S. C.; Akhuemonkhan, O.; Gaskell, K. J.; Wang, Q.; Frenkel, A. I.; Chu, D.; Salamanca-Riba, L. G.; Ehrman, S. H. Flame Synthesis of Nanosized Cu-Ce-O, Ni-Ce-O, and Fe-Ce-O Catalysts for the Water-Gas Shift (WGS) Reaction. *ACS Appl. Mater. Inter.* **2009**, *1* (11), 2624−2635.

(3) Trovarelli, A. Catalytic Properties of Ceria and CeO2-Containing Materials. *Catal. Rev.* **1996**, *38* (4), 439−520.
(4) Murray, E. P.; Tsai, T.; Barnett, S. A. A Direct-Methane Fuel Cell with a Ceria-Based Anode. *Nature* **1999**, *400* (6745), 649−651.
(5) Yahiro, H.; Baba, Y.; Eguchi, K.; Arai, H. High-Temperature Fuel-Cell with Ceria-Yttria Solid Electrolyte. *J. Electrochem Soc.* **1988**, *135* (8), 2077−2080.
(6) Imanaka, N.; Masui, T.; Hirai, H.; Adachi, G. Amorphous Cerium-Titanium Solid Solution Phosphate as a Novel Family of Band Gap Tunable Sunscreen Materials. *Chem. Mater.* **2003**, *15* (12), 2289−2291.
(7) Feng, X. D.; Sayle, D. C.; Wang, Z. L.; Paras, M. S.; Santora, B.; Sutorik, A. C.; Sayle, T. X. T.; Yang, Y.; Ding, Y.; Wang, X. D.; Her, Y. S. Converting Ceria Polyhedral Nanoparticles into Single-Crystal Nanospheres. *Science* **2006**, *312* (5779), 1504−1508.
(8) Hirano, M.; Kato, E. Hydrothermal Synthesis of Nanocrystalline Cerium(IV) Oxide Powders. *J. Am. Ceram Soc.* **1999**, *82* (3), 786−788.
(9) Li, H.; Lu, G.; Dai, Q.; Wang, Y.; Guo, Y.; Guo, Y. Hierarchical Organization and Catalytic Activity of High-Surface-Area Mesoporous Ceria Microspheres Prepared via Hydrothermal Routes. *ACS Appl. Mater. Inter.* **2010**, *2* (3), 838−846.
(10) Zawadzki, M. Preparation and Characterization of Ceria Nanoparticles by Microwave-Assisted Solvothermal Process. *J. Alloy Compd.* **2008**, *454* (1-2), 347−351.
(11) Djuricic, B.; Pickering, S. Nanostructured Cerium Oxide: Preparation and Properties of Weakly-Agglomerated Powders. *J. Eur. Ceram. Soc.* **1999**, *19* (11), 1925−1934.
(12) Kamruddin, M.; Ajikumar, P. K.; Nithya, R.; Tyagi, A. K.; Raj, B. Synthesis of Nanocrystalline Ceria by Thermal Decomposition and Soft-Chemistry Methods. *Scripta Mater.* **2004**, *50* (4), 417−422.
(13) Chu, X.; Chung, W. I.; Schmidt, L. D. Sintering of Sol-Gel-Prepared Submicrometer Particles Studied by Transmission Electron-Microscopy. *J. Am. Ceram. Soc.* **1993**, *76* (8), 2115−2118.
(14) Matijevic, E.; Hsu, W. P. Preparation and Properties of Monodispersed Colloidal Particles of Lanthanide Compounds.1. Gadolinium, Europium, Terbium, Samarium, and Cerium(III). *J. Colloid Interface Sci.* **1987**, *118* (2), 506−523.
(15) Nabavi, M.; Spalla, O.; Cabane, B. Surface-Chemistry of Nanometric Ceria Particles in Aqueous Dispersions. *J. Colloid Interface Sci.* **1993**, *160* (2), 459−471.
(16) Hsu, W. P.; Ronnquist, L.; Matijevic, E. Preparation and Properties of Monodispersed Colloidal Particles of Lanthanide Compounds.2. Cerium(IV). *Langmuir* **1988**, *4* (1), 31−37.
(17) Kim, S. K.; Paik, U.; Oh, S. G.; Park, Y. K.; Katoh, T.; Park, J. G. Effects of the Physical Characteristics of Cerium Oxide on Plasma-Enhanced Tetraethylorthosiliate Removal Rate of Chemical Mechanical Polishing for Shallow Trench Isolation. *Jpn. J. Appl. Phys. 1* **2003**, *42* (3), 1227−1230.
(18) Hirano, M.; Fukuda, Y.; Iwata, H.; Hotta, Y.; Inagaki, M. Preparation and Spherical Agglomeration of Crystalline Cerium(IV) Oxide Nanoparticles by Thermal Hydrolysis. *J. Am. Ceram. Soc.* **2000**, *83* (5), 1287−1289.
(19) Qi, L.; Sehgal, A.; Castaing, J. C.; Chapel, J. P.; Fresnais, J.; Berret, J. F.; Cousin, F. Redispersible Hybrid Nanopowders: Cerium Oxide Nanoparticle Complexes with Phosphonated-PEG Oligomers. *ACS Nano* **2008**, *2* (5), 879−888.
(20) Sehgal, A.; Lalatonne, Y.; Berret, J. F.; Morvan, M. Precipitation-Redispersion of Cerium Oxide Nanoparticles with Poly(Acrylic Acid): Toward Stable Dispersions. *Langmuir* **2005**, *21* (20), 9359−9364.
(21) Artelt, C.; Schmid, H. J.; Peukert, W. On the Impact of Accessible Surface and Surface Energy on Particle Formation and Growth from the Vapour Phase. *J. Aerosol Sci.* **2005**, *36* (2), 147−172.
(22) Tabakova, T.; Boccuzzi, F. B.; Manzoli, M.; Andreeva, D. FTIR Study of Low-Temperature Water-Gas Shift Reaction on Gold/Ceria Catalyst. *Appl. Catal. A−Gen.* **2003**, *252* (2), 385−397.
(23) Kundakovic, L.; Mullins, D. R.; Overbury, S. H. Adsorption and Reaction of H2O and CO on Oxidized and Reduced Rh/CeOx(111) Surfaces. *Surf. Sci.* **2000**, *457* (1−2), 51−62.
(24) Wang, X. Q.; Rodriguez, J. A.; Hanson, J. C.; Gamarra, D.; Martinez-Arias, A.; Fernandez-Garcia, M. In situ Studies of the Active Sites for the Water Gas Shift Reaction over Cu-CeO2 Catalysts: Complex Interaction Between Metallic Copper and Oxygen Vacancies of Ceria. *J. Phys. Chem. B* **2006**, *110* (1), 428−434.
(25) Tsunekawa, S.; Sivamohan, R.; Ito, S.; Kasuya, A.; Fukuda, T. Structural Study on Monosize CeO2-x Nano-particles. *Nanostruct Mater.* **1999**, *11* (1), 141−147.
(26) Perdew, J. P.; Wang, Y. Accurate and Simple Analytic Representation of the Electron-Gas Correlation-Energy. *Phys. Rev. B* **1992**, *45* (23), 13244−13249.
(27) Cook, L. M. Chemical Processes in Glass Polishing. *J. Non-Cryst. Solids* **1990**, *120* (1-3), 152−171.
(28) Hackley, V. A.; Paik, U.; Kim, B. H.; Malghan, S. G. Aqueous Processing of Sintered Reaction-Bonded Silicon Nitride.1. Dispersion Properties of Silicon Powder. *J. Am. Ceram Soc.* **1997**, *80* (7), 1781−1788.
(29) Jung, H. S.; Lee, J. K.; Lee, S.; Hong, K. S.; Shin, H. Acid Adsorption on TiO2 Nanoparticles - An Electrochemical Properties Study. *J. Phys. Chem. C* **2008**, *112* (22), 8476−8480.
(30) Goodman, A. L.; Bernard, E. T.; Grassian, V. H. Spectroscopic Study of Nitric Acid and Water Adsorption on Oxide Particles: Enhanced Nitric Acid Uptake Kinetics in the Presence of Adsorbed Water. *J. Phys. Chem. A* **2001**, *105* (26), 6443−6457.
(31) Wu, N. C.; Shi, E. W.; Zheng, Y. Q.; Li, W. J. Effect of pH of Medium on Hydrothermal Synthesis of Nanocrystalline Cerium(IV) Oxide Powders. *J. Am. Ceram Soc.* **2002**, *85* (10), 2462−2468.
(32) Wang, Y. M.; Wu, Z. Y.; Zhu, J. H. Surface Functionalization of SBA-15 by the Solvent-Free Method. *J. Solid State Chem.* **2004**, *177* (10), 3815−3823.
(33) Rocha, R. A.; Muccillo, E. N. S. Physical and Chemical Properties of Nanosized Powders of Gadolinia-Doped Ceria Prepared by the Cation Complexation Technique. *Mater. Res. Bull.* **2003**, *38* (15), 1979−1986.
(34) Zhang, Z. F.; Yu, L.; Liu, W. L.; Song, Z. T. Surface Modification of Ceria Nanoparticles and Their Chemical Mechanical Polishing Behavior on Glass Substrate. *Appl. Surf. Sci.* **2010**, *256* (12), 3856−3861.
(35) Cabot, B.; Foissy, A. Reversal of the Surface Charge of a Mineral Powder: Application to Electrophoretic Deposition of Silica for Anticorrosion Coatings. *J. Mater. Sci.* **1998**, *33* (15), 3945−3952.
(36) Suphantharida, P.; Osseo-Asare, K. Cerium oxide slurries in CMP. Electrophoretic Mobility and Adsorption Investigations of Ceria/Silicate interaction. *J. Electrochem Soc.* **2004**, *151* (10), G658−G662.
(37) Hingston, F. J.; Atkinson, R. J.; Posner, A. M.; Quirk, J. P. Specific Adsorption of Anions. *Nature* **1967**, *215* (5109), 1459−1461.
(38) Hingston, F. J.; Raupach, M. Reaction Between Monosilicic Acid and Aluminium Hydroxide.I. Kinetics of Adsorption of Silicic Acid by Aluminium Hydroxide. *Aust. J. Soil Res.* **1967**, *5* (2), 295−309.
(39) Hingston, F. J.; Quirk, J. P.; Posner, A. M. Anion Adsorption by Goethite and Gibbsite.1. Role of Proton in Determining Adsorption Envelopes. *J. Soil Sci.* **1972**, *23* (2), 177−192.
(40) Langmuir, I. The Constitution and Fundermental Properties of Solids and Liquids. Part I. Solids. *J. Am. Chem. Soc.* **1916**, *38* (11), 2221−2295.
(41) Basar, C. A. Applicability of the Various Adsorption Models of Three Dyes Adsorption onto Activated Carbon Prepared Waste Apricot. *J. Hazard Mater.* **2006**, *135* (1-3), 232−241.
(42) Dandu, P. R. V.; Peethala, B. C.; Babu, S. V. Role of Different Additives on Silicon Dioxide Film Removal Rate during Chemical Mechanical Polishing Using Ceria-Based Dispersions. *J. Electrochem Soc.* **2010**, *157* (9), Ii869−Ii874.
(43) Kelsall, A. Cerium Oxide as a Mute to Acid Free Polishing. *Glass Technol.* **1998**, *39* (1), 6−9.
(44) Dandu, P. R. V.; Devarapalli, V. K.; Babu, S. V. Reverse Selectivity - High Silicon Nitride and Low Silicon Dioxide Removal Rates Using Ceria Abrasive-Based Dispersions. *J. Colloid Interface Sci.* **2010**, *347* (2), 267−276.

(45) Karakoti, A. S.; Singh, S.; Kumar, A.; Malinska, M.; Kuchibhatla, S. V. N. T.; Wozniak, K.; Self, W. T.; Seal, S. PEGylated Nanoceria as Radical Scavenger with Tunable Redox Chemistry. *J. Am. Chem. Soc.* **2009**, *131* (40), 14144−14145.
(46) Asati, A.; Santra, S.; Kaittanis, C.; Nath, S.; Perez, J. M. Oxidase-Like Activity of Polymer-Coated Cerium Oxide Nanoparticles. *Angew. Chem. Int. Edit* **2009**, *48* (13), 2308−2312.
(47) Seo, Y. J.; Kim, G. U.; Lee, W. S. Effects of STI-Fill Thickness on the CMP Process Defects. *Microelectron. Eng.* **2004**, *71* (2), 209−214.
(48) Singh, R. K.; Bajaj, R. Advances in Chemical-Mechanical Planarization. *MRS Bull.* **2002**, *27* (10), 743−751.
(49) Basim, G. B.; Adler, J. J.; Mahajan, U.; Singh, R. K.; Moudgil, B. M. Effect of Particle Size of Chemical Mechanical Polishing Slurries for Enhanced Polishing with Minimal Defects. *J. Electrochem Soc.* **2000**, *147* (9), 3523−3528.
(50) Blaakmeer, J.; Bohmer, M. R.; Stuart, M. A. C.; Fleer, G. J. Adsorption of Weak Polyelectrolytes on Highly Charged Surfaces - Poly(Acrylic Acid) on Polystyrene Latex with Strong Cationic Groups. *Macromolecules* **1990**, *23* (8), 2301−2309.